PNAS RESEARCH ARTICLE | ENGINEERING

Programmable soft valves for digital and analog control

Colter J. Decker[a,b], Haihui Joy Jiang[a], Markus P. Nemitz[c], Samuel E. Root[a], Anoop Rajappan[b], Jonathan T. Alvarez[d], Jovanna Tracz[a], Lukas Wille[a], Daniel J. Preston[b,1], and George M. Whitesides[a,1]

Edited by John Rogers, Northwestern University, Evanston, IL; received April 14, 2022; accepted August 11, 2022

In soft devices, complex actuation sequences and precise force control typically require hard electronic valves and microcontrollers. Existing designs for entirely soft pneumatic control systems are capable of either digital or analog operation, but not both, and are limited by speed of actuation, range of pressure, time required for fabrication, or loss of power through pull-down resistors. Using the nonlinear mechanics intrinsic to structures composed of soft materials—in this case, by leveraging membrane inversion and tube kinking—two modular soft components are developed: a piston actuator and a bistable pneumatic switch. These two components combine to create valves capable of analog pressure regulation, simplified digital logic, controlled oscillation, nonvolatile memory storage, linear actuation, and interfacing with human users in both digital and analog formats. Three demonstrations showcase the capabilities of systems constructed from these valves: 1) a wearable glove capable of analog control of a soft artificial robotic hand based on input from a human user's fingers, 2) a human-controlled cushion matrix designed for use in medical care, and 3) an untethered robot which travels a distance dynamically programmed at the time of operation to retrieve an object. This work illustrates pathways for complementary digital and analog control of soft robots using a unified valve design.

untethered soft robotics | programmable devices | analog control | digital logic | nonlinear mechanics

Significance

We designed soft pneumatic valves to allow complex sequences of actuation and precise control of forces in both digital and analog formats. These valves leverage the nonlinear mechanics of soft materials. Based on this design, we created systems capable of analog pressure regulation, linear actuation, digital logic, pressure amplification, controlled oscillation, nonvolatile memory storage, and interfacing with human users. Combining digital and analog components enables control circuits with significantly fewer physical valves compared to equivalent, but strictly digital, circuits. The programmability of these valves (i.e., with tunable pressures of actuation and output) simplifies the operation of multipressure systems, helping to untether robots and create intuitive, human-friendly devices.

1. Introduction

As the field of soft robotics evolves, devices are becoming increasingly complex. Soft and semisoft pneumatic robots can now execute challenging actions including beating video games (1), playing piano (2), and navigating uncertain environments (3, 4). This advancement in soft devices brings more effective medical care, with examples such as devices for the rehabilitation of hands that track complex thumb motions and robots capable of minimally invasive endoscopic surgery on a beating heart (5, 6). Other developments include increasingly general object manipulation capabilities (7, 8) and closer ties between humans and robots (9–11). However, many soft device control systems still rely on hard valves and electrical control components (12, 13). Recent work suggests the integration of control systems into soft devices is a necessary step to enable complex devices and difficult actuation sequences while maintaining the advantages that soft materials provide (14–18).

Early fluidic logic, primarily implemented through microfluidics (19–21), represents a step in this direction. The scalability of the Quake valve has allowed researchers to incorporate thousands of fluidic logic elements in a single device (22). More recently, Wehner et al. (23) leveraged a microfluidic logic system to fabricate a fully soft, untethered Octobot with oscillating arms. However, for most applications in soft robotics, slow flow rates (0.1 to 10 mL/min) restrict actuators to small scales of force (24–26). Furthermore, while modification of the fundamental system architecture could potentially enable efficient logic akin to complementary metal-oxide semiconductor (CMOS)–type systems (27), most microfluidic systems lose energy at steady state due to pull-down resistors, analogous to early transistor-transistor electronic logic systems.

Multiple recently developed soft valves have attempted to address the scale and flow rate limitations of microfluidics. Tracz et al. (28) proposed a tube-balloon logic (TBL) valve capable of functioning at pressures up to 200 kPa. Similarly, Lee et al. (29) have demonstrated a buckling-sheet valve that controls pressures up to 80 kPa. Both systems reach high frequencies when configured as ring oscillators (15 and 10 Hz, respectively) but are limited by pressure loss introduced by pull-down resistors; the ratio of oscillator output pressure to input pressure is 0.24 for the TBL oscillator and 0.76 for the buckling-sheet ring oscillator. Additionally, neither valve is bistable, meaning that a wide range of intermediate output pressures are feasible. This behavior can be desirable

Competing interest statement: G.M.W. acknowledges an equity interest and board position in Soft Robotics Inc. None of the work described in this article was connected to any present interest of Soft Robotics Inc.

This article is a PNAS Direct Submission.

[1]To whom correspondence may be addressed. Email: gwhitesides@gmwgroup.harvard.edu or djp@rice.edu.

This article contains supporting information online at http://www.pnas.org/lookup/suppl/doi:10.1073/pnas.2205922119/-/DCSupplemental.

Published September 26, 2022.

for continuous control but limits the ability of the valves to function in cascaded logic circuits.

The silicone kink valves proposed by Rothemund et al. (30) successfully addressed many of the limitations of microfluidic logic systems. These valves reach pressures of 45 to 50 kPa before material failure occurs, require only a single high-pressure source, and—due to their implementation of CMOS-type logic—do not lose energy at steady state to pull down resistors. These advances led to the demonstration of several capabilities at a scale appropriate for soft robotics, including cascaded digital logic (4), single-input ring oscillators (31), nonvolatile memory storage (32), and built-in environmental navigation capabilities for an untethered robot (3). However, several key challenges remain. Fluidic logic elements composed of silicones necessitate long curing times, require new molds for each design iteration, and are cumbersome to repair or modify. Operational pressure ranges still limit use cases to relatively low-pressure actuators, and oscillation speeds have not been demonstrated at frequencies faster than 0.3 Hz in CMOS-type valves, although non-CMOS designs have been shown to oscillate more quickly and require less energy.

Researchers have attempted to harness multimaterial three-dimensional (3D) printing technologies to overcome the limitations of both microfluidic Quake valves (33) and macroscale elastomeric soft valves (1), but many limitations of early fluidic logic systems persist. Current 3D printed valves require pull-down resistors to function, meaning cascaded fluidic logic circuits become energetically expensive. Larger valves employ hard components, limiting their use in wearable devices. Furthermore, while automated manufacturing reduces the need for human labor, timescales for fabrication are still on the order of days (1). Long fabrication times combined with the cost and limited accessibility of multimaterial 3D printing restrict the scalability of this process. The monolithic nature of 3D printing also means repairing or reconfiguring devices would be prohibitive; even in the prototyping stage, this approach may not be time or labor effective.

Components that simplify actuation sequences without establishing a functionally complete set of logic elements have also been developed. For example, viscous flow can be used to set actuation timing delays (34, 35). Viscous flow has also been considered in designing a collection of valves to create a set of passive control elements (36). Meanwhile, fluidic digital information transfer and storage schemes—including a fluidic demultiplexer (37) and random-access memory (38)—represent important steps toward simplified fluidic control in soft devices but still require electronic controllers when they are not paired with a complementary set of fluidic logic elements (4).

Furthermore, absent in all the aforementioned systems is analog pressure regulation (highlighted in Table 1, along with other details on the state of the art). A previous step toward analog control consisted of a pneumatic digital-to-analog converter built with 12 digital valves (4) capable of outputting four distinct pressure levels, but this device required a separate pressure input line for each level. No digital circuit can ever be entirely analog in nature, and more accurate approximations require an increasing number of physical valves. More recently, a pressure regulator was designed from Quake-like valves (27); this design also required multiple pressure inputs, and its function was limited to controlling the hysteresis of other valves.

Developing a general pressure regulator for soft devices would enable four significant advances in soft control capabilities. The first advance is the development of combined analog and digital control circuits. Previous advances in methods of controlling soft devices have focused primarily on either digital circuits (which can achieve high levels of computational complexity at the cost of space and time) or analog circuits (which can realize simple functions like actuation delays with few components but are not generalizable to a range of desired behaviors). The addition of an analog regulator to a suite of digital valves would allow the creation of highly functional, complex, and generalizable combined digital-analog circuits, minimizing the time, space, and pressure requirements of a control system. The second advance that would be enabled is the simplification of control systems. Previously, multiple input lines were necessary when logical elements and actuators required different operating pressures. A pressure regulator simplifies the design by enabling multiple, separate output pressures from the same input line. Third, a pressure regulator represents a step toward untethered soft robots. Fully untethered soft pneumatic robots must carry their pressure supply. Reaching acceptable energy densities was previously achieved through chemical reactions (23) or pressurized fluids (3, 40). For pressurized fluids, pressure regulators composed of rigid materials were required to lower the supply pressure; a compliant pressure regulator could, in the future, replace this hard component. Finally, rigid analog pressure regulators are routinely used to obtain human input (e.g., by manually adjusting a control knob to change the behavior or state of a soft robot). The development of a lightweight regulator composed of compliant materials would allow safer and easier interaction with users, especially in wearables.

This work describes a programmable control system that takes advantage of the nonlinear mechanics of membrane inversion and tube kinking of soft materials. Composed of two modular devices—a piston actuator (Fig. 1*A*) and a mechanically actuated switch (Fig. 1*B*)—the compliant valves we developed are capable of digital logic control, analog pressure control, nonvolatile memory storage, and interpretation of human and environmental inputs in both digital and analog formats. Two examples of useful combined digital-analog circuits demonstrated in this work are a counter circuit and a ring oscillator with the built-in capability for an adjustable oscillation frequency. Our work improves upon the functionality of previous devices through the following unique combination of seven achievements (Table 1): 1) introducing analog control capabilities; 2) implementing CMOS-type logic to avoid energy loss at a steady state; 3) increasing maximum operating pressure to more than 165 kPa for digital CMOS-type valves (*SI Appendix*, section 16); 4) consequently increasing the response time of the valves, which corresponds to a 10x increase in ring oscillation frequency (from 0.3 to 3 Hz when considering CMOS-type valves); 5) reducing the fabrication time to less than 12 min and reducing the material cost to less than US$ 0.40 per valve (calculated in *SI Appendix*, Table S1); 6) enabling valves to be repaired and reconfigured easily; and 7) reducing the number of physical valves needed to build digital logic circuits by introducing previously unreported pneumatic logic gates—inhibition (INHIB), implication (IMPLY), and a three-input gate—and combined digital and analog control circuits.

2. Results

2.1. Design. We designed two modular soft components: a linear actuator (Fig. 1*A*) and a bistable, mechanically actuated switch (Fig. 1*B*). The piston-like linear actuator employs a rolling diaphragm fabricated from a flexible film. Rolling diaphragms have been used in both linear and rotational hard pistons (41, 42) to remove energy loss from friction while maintaining a fluid-tight

Table 1. Broad comparison of our valves with previous methods of soft device control

Capability	Our valves	Bistable silicone valves (3, 4, 30, 31)	Buckling-sheet logic (29)	Tube-balloon logic (28)	Microfluidics (24, 25, 39)	Flow-based control (36)
CMOS-type	✓	✓	—	—	—	✓
High-pressure tolerances	✓	—	—	✓	✓	✓
Practical flow rates for actuation	✓	✓	✓	✓	—	✓
Fast, inexpensive fabrication	✓	—	✓	✓	✓	✓
High oscillation frequencies	✓	—	✓	✓	✓	—
Analog control capabilities	✓	—	—	—	—	—
Nonvolatile memory	✓	✓	—	—	✓	—
Programmable snap-through	✓	—	—	—	—	—

seal (43), but they have seen limited adoption due to constraints surrounding fabrication of long diaphragms (41). Methods to create long rolling diaphragms have been proposed, but they are intensive and none are commercially available (41, 44, 45). By heat sealing two layers of thermoplastic polyurethane (TPU) separated by parchment paper, we are able to fabricate rolling diaphragms with arbitrary geometry. Using lightweight polypropylene straws (used as tubes for drinking consumer beverages) as inner and outer piston chambers secured to the diaphragm (*SI Appendix*, section 1), we create a simple pneumatic piston (Fig. 1*A*). This piston functions independently as a linear actuator or as a modular component to be combined with other soft devices explored in this work.

To develop the mechanically actuated pneumatic switch (Fig. 1*B*), we use an elastic tube with two polypropylene drinking straws. The elastic tubing is threaded between the two straws and secured with fast-drying glue (full fabrication instructions are listed in *SI Appendix*, section 2). In the initial state, one soft tube is kinked while the other is extended to allow flow. A net force above a critical value of 0.5 N causes the inner straw to translate with respect to the outer straw and alternate which of the two soft tubes is kinked. The kinking of the tube is the result of a nonlinear mechanical instability: this snap-through phenomenon is bistable, meaning that the tube will remain in the kinked position when the force is released. Likewise, a net force of 0.5 N applied in the opposite direction will return the switch to its original state. The snap-through force must be large enough to maintain switch bistability but should be low enough that the switch easily transitions between states. This force is theoretically tunable by altering tube material and geometry, but a force of 0.5 N satisfies both conditions. The switch can be used alone as a button for humans to reprogram and control pneumatic circuits, and it could also be used to detect obstacles or obtain other environmental information.

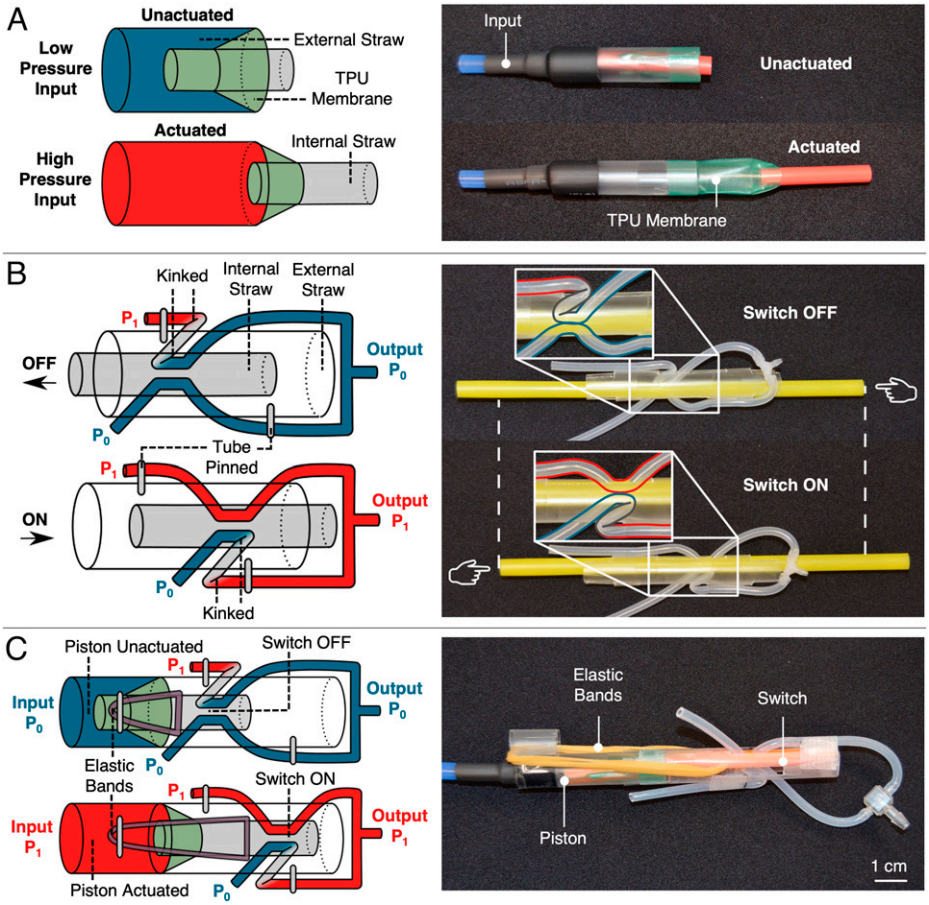

Fig. 1. Soft piston, switch, and valve. (*A*) Schematics and photos of the soft piston actuator. (*B*) Schematics and photos of a mechanically actuated pneumatic switch. (*C*) Piston actuator combined with the mechanical switch and an external elastic band, forming a pneumatic valve.

Instead of using two separate interior polypropylene straws—one as the piston head and one inside of the switch—the two components can be combined by using a single straw as an interface (*SI Appendix*, section 3). The resulting device is a valve composed of lightweight, compliant materials. The piston translates a pneumatic input into a mechanical force acting on the switch. Once pressure reaches the critical snap-through force per unit area, the switch rapidly changes states. We restrain the switch with elastic bands, which converts the bistable system to a monostable one when no pressure is applied. Therefore, the resulting device is a valve that switches between two states depending on applied pressure (Fig. 1*C*). The snap-through pressure is determined by the stiffness of elastic bands used, introducing programmability to the valves. Further discussion of valve stability can be found in *SI Appendix*, section 6.

Three valves were tested to 10,000 cycles each before an elastic band failed on one valve. This externally attached elastic band can be easily swapped without refabrication of the entire device. Our method of fabrication is rapid (requiring less than 12 min) and inexpensive (less than US$ 0.40 per valve) compared to existing molded silicone and 3D printed valves, which require hours to cure or print (1, 30).

2.2. Tunability. When configured as a valve (Fig. 2*A*), multiple forces act on the inner switching straw. Pressure applied to the piston head balances the opposing elastic tension and friction from the system in the base state (Fig. 2*B*). When these forces sum to the critical value of 0.5 N, the switch snaps through (i.e., the inner straw moves to the right). Returning to the base state requires a net force of 0.5 N in the opposite direction, creating a region of hysteresis. Changing elastic stiffness affects the pressure at which this net force is reached and shifts the snap-through and snap-back pressures (Fig. 2*C*). Consequently, the operating pressure of the valve can be tuned based on the intended application. For example, the valve can control pressures significantly higher than the input pressures it receives. This behavior enables logic cascading and pressure amplification (30).

By individually characterizing the force on each component, we create a model to predict valve snap-through pressures as a function of elastic stiffness (*SI Appendix*, section 9). Elastic, piston, and frictional forces are modeled analytically as functions of switch displacement, elastic stiffness, and input pressure. Tube kinking is modeled empirically by measuring the behavior of the switch in isolation. When the valve snaps forward, frictional, elastic, and tube kinking forces all oppose the applied piston force, which yields a force-balance equation and allows us to determine snap-through pressures. When the valve snaps back, the elastic force opposes piston, frictional, and tube kinking forces, which gives a separate force-balance equation. The semiempirical physical model applied in this work agrees with experimental results (Fig. 2*D*). This quantitative correlation enables programmability with precision and control. In implementations of digital logic, the model could guide design of snap-through pressures between two threshold values corresponding to Boolean 0 and 1; for analog systems; on the other hand, this tunability allows real-time regulation of setpoint pressures.

2.3. Digital Control. The bistable nature of this valve allows it to manipulate digital values without ambiguity. After assigning logical values to high- and low-pressure states, this valve can compute Boolean computer logic. Since pressure outputs can switch between two entirely different sources, CMOS-type logic

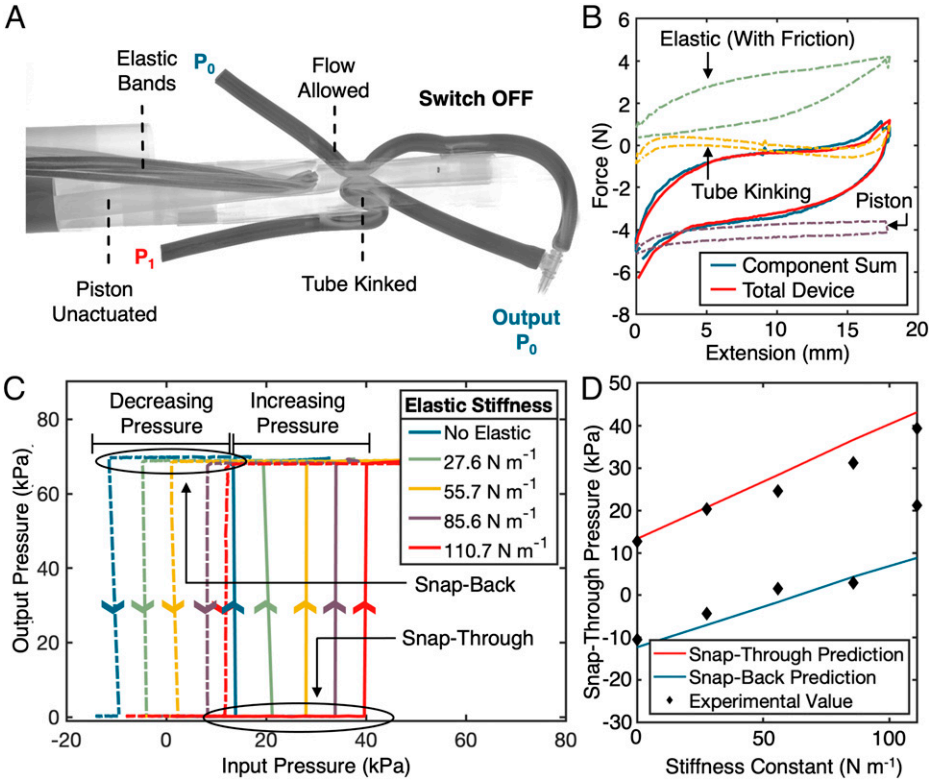

Fig. 2. Tunable valve. (*A*) Micro-computed tomography (micro-CT) image of the bistable valve configured as a pneumatic switch. (*B*) Force-distance curves of different device components. In this case, the switch uses elastics with k = 110.7 N m^{-1} and a piston pressurized to 80 kPa. (*C*) Snap-through and snap-back pressures of the pneumatic valve with different elastic stiffness constants (*k*, in units of N m^{-1}). Rapid changes in output pressure as a function of input pressure demonstrate the bistability of the valve. (*D*) We measure snap-through and snap-back pressures while varying elastic band stiffness. Experimentally measured valve snap-through and snap-back pressures for the valve (solid black diamonds) compared with predictions from the semiempirical model (red and blue curves) show good agreement.

is possible (eliminating energy loss through pull-down resistors). Up to this point, it has been assumed the valve is configured with a high-pressure line connected to the initially kinked tube while the initially unkinked tube is open to atmospheric pressure. If we consider high pressure to represent Boolean 1 and atmospheric pressure to represent Boolean 0, then this valve mimics a noninverting Schmitt trigger. Specifically, the value of the high pressure representing Boolean 1 must be greater than the snap-through pressure of the valve. Because this snap-through pressure is tunable, the pressure value representing Boolean 1 might change depending on the intended application. From now on, Boolean 1 will refer to pressures between 30 and 75 kPa (used in different applications and demonstrations), while Boolean 0 will always refer to atmospheric pressure.

Under this framework, varying the inputs to the valve creates a variety of useful logic gates. For example, connecting constant atmospheric pressure (P_0) to the initially kinked tube with a constant source of high pressure (P_1) connected to the initially unkinked tube is analogous to a NOT gate (Fig. 3*A*). In this example, the piston chamber is the sole variable input to the gate; however, multiple tubes can be set as inputs to create two or three input logic gates. The set of AND and OR gates (Fig. 3 *B* and *C*), along with the NOT gate, is a functionally complete set of logic gates, meaning that any Boolean operation can be computed with enough gates and time (46). Previous soft pneumatic logic systems using this set of gates have successfully built set-reset (SR) latches, 2-bit shift registers, and digital-to-analog converters (4).

In practice, lowering the number of physical valves in a logic system ensures rapid actuation and low system volume (47). We achieve this goal with additional logic gates previously unreported in soft systems. A single INHIB gate (Fig. 3*E*) is equivalent to chaining a NOT gate to one input of an AND gate. Similarly, an IMPLY gate (*SI Appendix*, section 7) is equivalent to chaining a NOT gate into one input of an OR gate. Adding these gates to the set lowers the number of valves needed to create an exclusive OR (XOR) gate from five to three (*SI Appendix*, section 8). Additionally, considering all tubes on

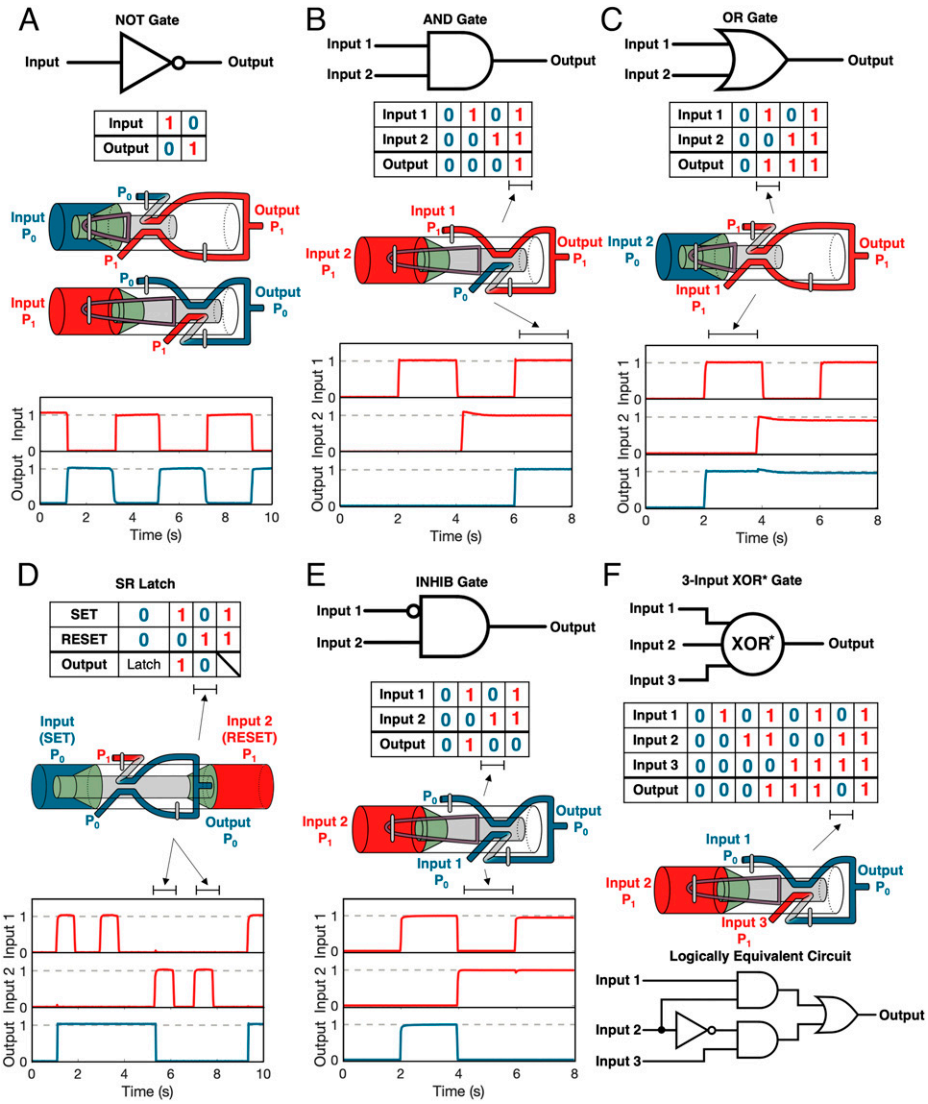

Fig. 3. Digital control using pneumatic logic gates. The bistable valve is arranged with different input connections to achieve logic gate behaviors. (*A*) A NOT gate is made by attaching supply pressure (Boolean 1) to the initially unkinked tube and atmospheric pressure (Boolean 0) to the initially kinked tube. (*B*) An AND gate is created by setting the piston chamber and initially kinked tube as inputs and connecting the initially unkinked tube to atmospheric pressure. (*C*) An OR gate is made by setting the piston chamber and initially unkinked tube as inputs while connecting the initially kinked tube to supply pressure. (*D*) SR latch schematic. The output is undefined when both inputs are 1. When both inputs are 0, the SR latch outputs the previous state, creating memory. (*E*) INHIB gate schematic. (*F*) Three-input XOR* gate schematic, along with the equivalent logic circuit. All gates were tested with a pneumatic 1 between 60 and 75 kPa.

the gates as variable inputs creates a three-input logic gate (Fig. 3*F*). We label this gate XOR*, as adding it to the previous set allows XOR and exclusive NOT OR (XNOR) gates to be constructed with just two valves.

Finally, adding a second pressure chamber to the opposite side of the valve and removing the elastic band causes the snap-back pressure to be negative, recovering the bistability observed in the elementary switch shown in Fig. 1*B*. The result is a single-valve SR latch (Fig. 3*D*). This SR latch retains its mechanical state even after the pressure source is removed, enabling nonvolatile memory using the same physical framework as the rest of the gates.

2.4. Analog Control. In addition to digital logic, this system is capable of analog pressure control. Removing (or blocking) the initially kinked tube present in the previous valve and feeding the output to the piston chamber creates a regulator (Fig. 4*A*). If the output pressure is high, the piston kinks the internal tube, limiting flow. The pressure at which a kink forms is determined by the balancing of force between the piston and the opposing force components (from the valve restraint, tube kinking, and friction). We include an inextensible string as the valve restraint instead of an elastic band to directly transfer a human user's force input to the piston head. Accordingly, by increasing the external pulling force applied to the string, one can raise the output pressure of the regulator (Fig. 4*B*).

Because this regulator is lightweight, durable, compliant, and outputs variable pressures, it is a good candidate for a wearable method of pneumatic control. To demonstrate its suitability in a wearable device, we fabricated a glove with five embedded regulators, each connected to a different finger (Fig. 4*C*). This glove controls a soft robotic hand (Fig. 4*D*). The glove can hold any finger at any position between its maximum and minimum displacement (Fig. 4 *E* and *F*), a continuous form of control that digital pneumatic systems alone cannot achieve or even emulate without an infeasible number of logic elements. By tailoring the length of inextensible string, we matched the deflected angle of each robotic finger actuator to a human user's finger within 2° of deviation over a range of 0° to 130° (Fig. 4*G*, with detailed characterization over the full range of angular positions shown in *SI Appendix*, sections 11–12 and Fig. S13).

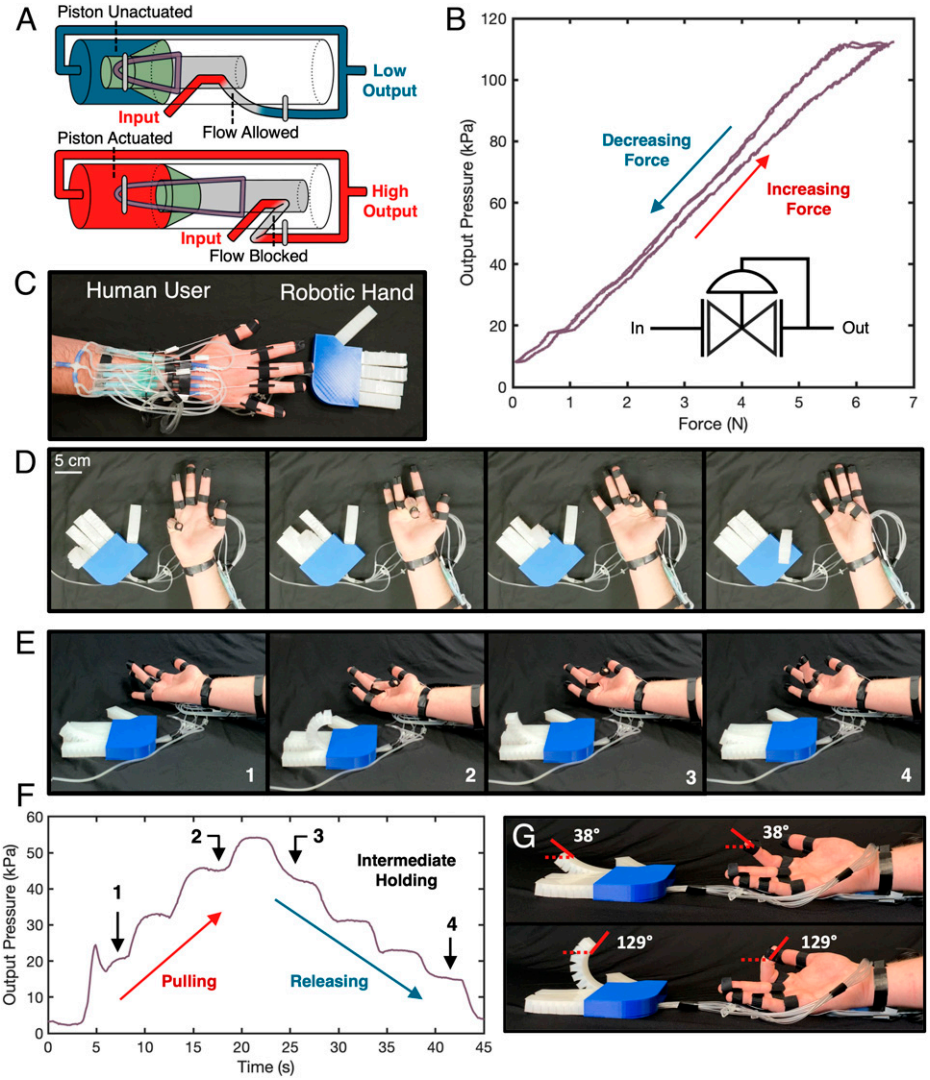

Fig. 4. Analog control using a soft pressure regulator. (*A*) Diagrams of the pressure regulator. If output pressure is too high, the valve restricts airflow. If output pressure is too low, the valve allows flow. (*B*) Regulator output pressure depending on input force. (*C*) Top view of the five-finger control glove and soft robotic hand with one soft actuator for each finger. The system is powered with a single constant pressure input. (*D*) Pressure regulator used as an analog human input with an analog control glove. Output pressure (which controls pneumatic devices, such as the soft robotic hand) varies as the string is pulled or released. (*E*) Holding the robotic hand between fully actuated and unactuated states. (*F*) Single actuator pressure measurements during device operation. (*G*) Angle of the analog finger actuator on the soft robotic hand tuned to correspond to the user's finger angle.

Apart from improving human-device interactions, this device is an important step toward fully untethered soft robots. A regulator can separate control systems and different actuators, allowing them to function at different pressures while all using a common source. Additionally, onboard high-pressure sources (up to the input limit for the regulator of 168 kPa) can be regulated down to more appropriate levels for actuation and control.

2.5. Combined Digital-Analog Logic Circuits.

2.5.1. An untethered soft robot. The component-level modularity discussed to this point allows development of devices for both digital logic and analog control to be fabricated using the same architecture. Going a step further, with device-level modularity, combined analog-digital circuits with complementary functions can be constructed. We demonstrate two examples of combined digital-analog circuits: a ring oscillator with a continuously varying output frequency (Fig. 5 *A*–*D*) and a reprogrammable counter circuit (Fig. 5 *E* and *F*). Both circuits could not be feasibly integrated in most soft devices using only digital components due to device size restrictions; *SI Appendix*, section 13 describes how a digital counter circuit would require 30 or more physical gates, in contrast to our approach based on an analog regulator, which reduces the number of gates required to fabricate a counter to only 6.

The ring oscillator is fabricated by arranging three NOT gates in a ring (Fig. 5 *A* and *B*), creating an instability in the system that results in an oscillatory output from a constant pressure input (46). Soft ring oscillators have previously been used to control mechanotherapeutic wearable devices (31) and untethered robots (3). Because the frequency of oscillation is highly dependent on input pressure (Fig. 5 *C* and *D*), an analog pressure regulator placed upstream from the oscillator can control oscillation frequency. In practice, one could use a regulator to change the speed of an untethered robot or adjust the oscillation frequency and force of a mechanotherapeutic device to maximize comfort and function.

Previous soft ring oscillators using CMOS-type architectures have reached frequencies of about 0.3 Hz (3, 31). However, there is a demonstrated need for higher-frequency oscillation in applications including haptics, communication, grasping, and reaching (48). Ring oscillators assembled from inverters that require pull-down resistors to function have reached frequencies of 10 to 15 Hz (28, 29). However, the loss of pressure inherent to architectures utilizing resistors limits the ratio of output

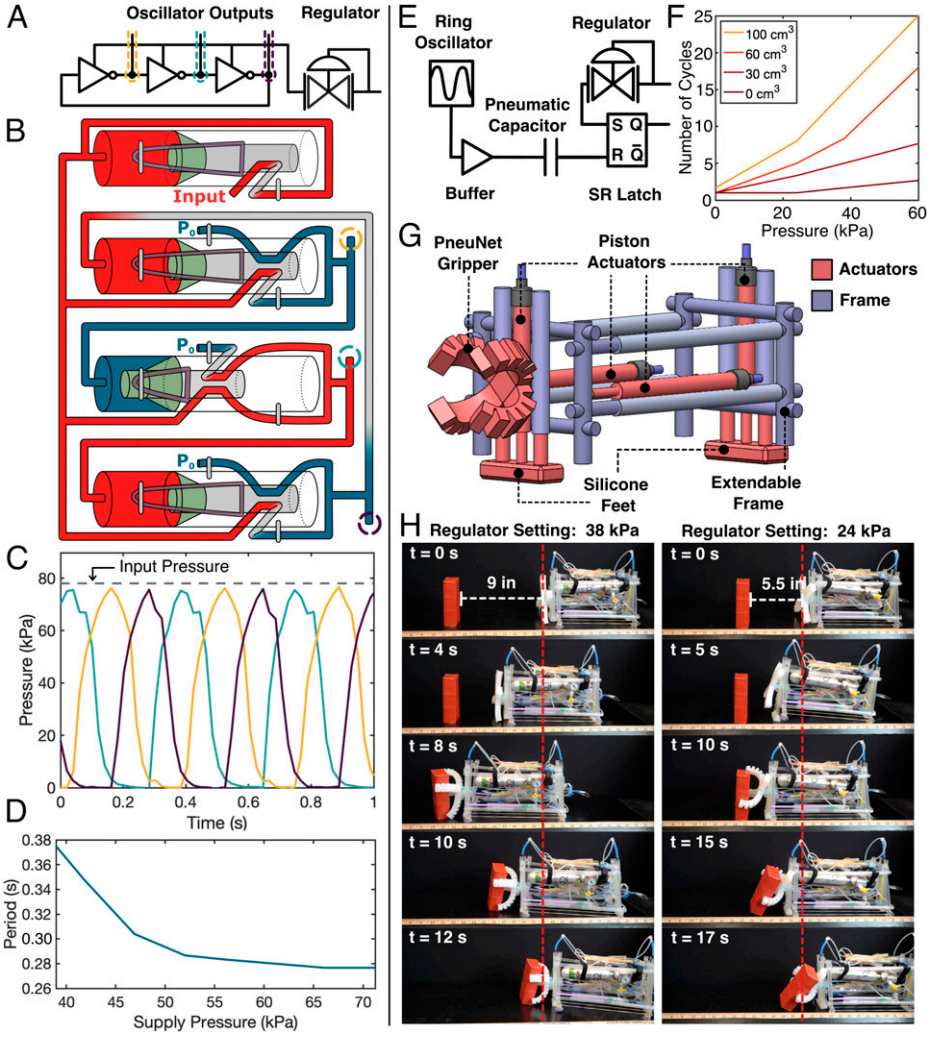

Fig. 5. Ring oscillator. (*A*) Schematic of the assembled ring oscillator logic circuit with a soft pressure regulator controlling input pressure. (*B*) Diagram of the regulator and oscillator circuit showing valve connections. (*C*) Pressure output from each gate with a constant pressure supply of 78 kPa. Maximum pressure output is 76 kPa, meaning only a 3% reduction in pressure occurs. (*D*) Period of oscillation at different supply pressures. (*E*) Schematic of the counter circuit. (*F*) Number of cycles before switching states at different capacitor volumes and regulator input pressures. (*G*) Diagram of untethered robot. (*H*) Robot retrieving an object at two different distances based on counter settings programmed dynamically at the time of deployment. The internal volume of the robot is 80 cm^3, yielding 11 and 7 stepping cycles for the 39- and 24-kPa deployments, respectively, based on the cycle programming data shown in *F*.

pressure to input pressure P_o/P_i; previous oscillators have demonstrated P_o/P_i ratios of 0.76 and 0.24. There is a growing body of work focusing on locomotive soft robots that use either 1) an oscillatory pressure input or 2) a constant pressure input that generates oscillation, which then translates to movement (3, 30, 31). Improvements in oscillation speed can directly increase locomotive speed. Due to the high operational pressures, quick snap-through times, and CMOS-type architecture, ring oscillators built with our proposed design can reach a P_o/P_i ratio of 0.97, as well as frequencies of up to 3.6 Hz, over 10 times faster than previous CMOS-type designs.

Building on the ring oscillator, we designed an integrated digital-analog circuit to count the number of oscillations in order to program time-dependent robot operation (Fig. 5*E*). The output of the ring oscillator connects to a buffer, which provides positive pressure when actuated without allowing any backward flow to the oscillator. This buffer incrementally pressurizes a pneumatic capacitor (i.e., a sealed, fixed volume) through a thin pneumatic resistor during each oscillation period. The capacitor in turn connects to the set input of an SR latch, which functions as a pressure comparator in this circuit. When the pressure on the side of the SR latch connected to the capacitor exceeds the pressure applied to the other side (which is provided by a regulator), the latch will snap through, indicating that a preset number of cycles has been reached. By changing the setting of the analog regulator, a human user can change the number of cycles (or length of time) counted (Fig. 5*F*). This combined digital-analog counter is theoretically infinitely adjustable, in the sense that the only limitation to the number of distinct settings is the quality of fabrication. *SI Appendix*, section 13 illustrates how a comparable digital-only circuit (with only eight possible settings) would require 30+ physical valves, instead of the six required in this circuit.

Combining the ring oscillator and counter circuit, we create a dynamically programmable untethered soft robot (Fig. 5*G*). Advances in control schemes for soft devices have led to robots which can walk, grab, and navigate environments (3, 49, 50). Such robots are generally inexpensive to produce, safe for interaction with humans and animals, and durable in harsh environments. The combination of these traits makes soft robotic technology appealing for use in search and rescue or exploration scenarios. However, many of these robots either require a tethered pressure source to function or are limited in capabilities due to weight and size constraints. Because the valves developed in this work are light (less than 5 g), they are good candidates for use in an untethered robot.

We demonstrate an untethered locomotive robot which can move forward, grasp an object, and return to its initial position (Fig. 5*H*). The forward distance traveled can be dynamically programmed by a human user at the time of deployment by adjusting the net tension in the elastic bands attached to the regulator portion of the analog counter circuit described above, which keeps track of the number of steps taken by the robot. In practice, the user would choose how many elastic bands attached to the regulator to leave in tension; different numbers of elastic bands correspond to different precalibrated distances. This demonstration marks an untethered soft robot that can be programmed dynamically at the time of deployment. Furthermore, robot locomotion is achieved by using the piston actuator as a standalone device, demonstrating its versatility and practicality outside of use as a soft valve. *SI Appendix*, section 14 details the robot construction, functionality, and control circuit in depth.

2.5.2. A multifunctional cushion matrix. To demonstrate another distinct capability of the pneumatic control system developed in this work, we fabricated a prototype of a cushion matrix (*SI Appendix*, section 15). The cushion is connected to a single pressure source, yet depending on which pneumatic switch is turned on, lifting, rolling, or oscillatory mechanotherapeutic functions can be activated (Fig. 6*A*). The rolling function (Fig. 6*B*) activates a column of cushions which could lift one side of a human and aid in, for example, patient repositioning. The lifting function (Fig. 6*C*) inflates a row of cushions near the head or feet. The oscillation function sequentially inflates and deflates pairs of pouches. Control of each function is realized by connecting pouches with a series of OR gates, which are necessary to prevent flow between pouches that should remain deflated. A regulator controls the actuation pressure of each function, as well as the frequency of oscillation.

As an alternative to this integrated digital-analog control unit, a human user can directly control different sets of pouches using only our analog control glove (Fig. 6*E*). We show a use case in which the thumb, index finger, and middle finger are used to control the top, middle, and bottom pairs of actuators, respectively, on the cushion matrix. The degree of deflection of the thumb and fingers serves as a method to achieve continuous control of the pressure to which each pair of pouches is inflated. In addition to applications in patient lifting and mechanotherapy, the incorporation of direct analog control of these three regions on the cushion matrix offers promise for emotional interaction with patients in quarantine or under other restrictions regarding interaction with medical professionals, building on work such as the soft HugBot (51) and related haptic approaches, which have been shown to be preferred by humans compared to rigid alternatives (52). Future iterations of our glove and cushion matrix could even complement systems which also apply heat in human interaction and emotional connection (53).

A scaled-up version of this cushion matrix could aid medical professionals who require physical assistance in repositioning patients in medical settings, including elevating body parts or moving. Such a device might also reduce the number of work-related injuries in hospitals; 253,700 injuries caused lost work time in 2011 (higher rates than both construction and manufacturing industries), and 48% of these injuries were due to overexertion, often in relation to maneuvering patients (54). Because hospital rooms are typically equipped with an in-house pressure source, they are logical candidates for use of a scaled-up version of this device. However, the proposed cushion matrix could be used on any bed with a suitable supply of pressurized air (e.g., in nursing homes or for at-home comfort) and is not limited to hospitals.

3. Conclusion

In addition to improved logic gate functionality (greater than 165-kPa maximum pressure and 10 times faster oscillation frequencies compared to previous CMOS-type valves), the valves presented in this paper bring several higher-level advantages relative to other approaches already reported (3, 4, 28, 29). The modularity of our valves means that a wide range of functions (digital and analog control, nonvolatile memory, linear actuation, and human-operated pneumatic switches) can all be achieved using largely the same soft device design and fabrication process. This simplicity leads to faster prototyping times—existing components can easily be recombined or reconfigured into different devices—but it is also an important step toward enabling large-scale production and adoption of complex soft devices.

Beyond the aforementioned advantages, analog pressure regulation is a unique benefit of this system. Analog pressure regulation

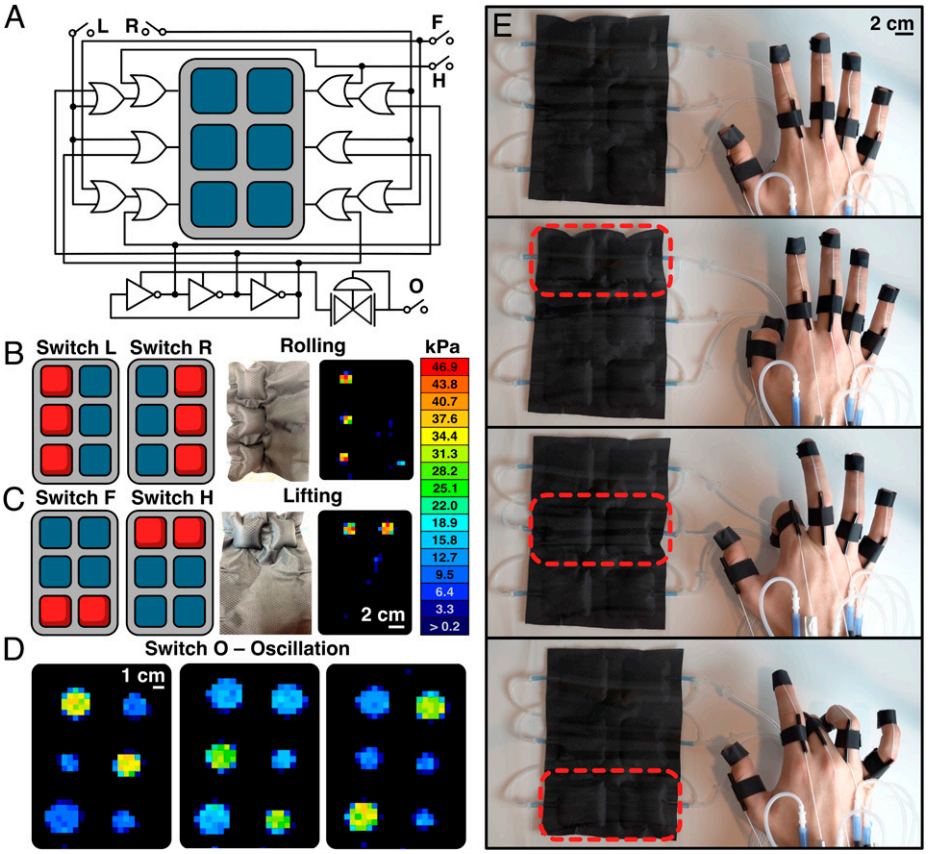

Fig. 6. Multifunctional pneumatic cushion. (*A*) Logical circuit used with the cushion matrix. Five switches, each with individual functions—left (L), right (R), feet (F), head (H), and oscillate (O)—are labeled. (*B* and *C*) Visualization of the rolling and lifting functions of the matrix, with schematics, pictures, and experimental pressure measurements. (*D*) Experimental pressure measurements of the cushion while the oscillation function is activated. The prototype was operated with an input pressure of 70 kPa. The cushion is restrained with a transparent acrylic sheet to simulate the weight of a user. Two-dimensional pressure maps are shown (with orange-red representing high-pressure outputs and blue-black representing low-pressure outputs). (*E*) Direct analog control of the pneumatic cushion. Red boxes show pouches that are being inflated.

expands the capabilities of soft devices by reducing the number of necessary input lines to multipressure systems, helping untether soft robots, creating intuitive human-robot interactions, and enabling combined digital-analog circuits. The inherent programmability of these devices represents another important advantage. At the component level, the snap-through pressures of the valve and output pressure of the analog regulator can easily be set. At the system level, the kinking and membrane inversion mechanisms presented in this paper are general concepts that can be transferred to other materials (e.g., plastics and fabrics) and scales depending on application needs.

Despite these advances, the field of soft device control still presents several directions for future work building on this valve architecture. Fabricating valves by hand will always introduce variability in function. While this limitation is not a major issue when constructing small pneumatic circuits, complex cascaded logic could require higher precision, especially in the case of analog circuits. Developing an automated valve fabrication process would increase precision while simultaneously lowering fabrication time and human effort. Future work could also include material and dimensional optimization with the goals of higher durability, more pronounced bistability, and higher pressure tolerances. However, even in its present form, the valve design presented in this work addresses critical limitations in the field. We introduce a single valve architecture capable of simultaneous digital and analog control. Implementation of CMOS-type logic avoids energy loss at a steady state, and the fabrication time and cost have been reduced to less than 12 min and less than US$ 0.40, respectively. Compared to previous valves capable of CMOS-type logic, the maximum operating pressure is increased by more than 300%; this change consequently improves the response time of the valves, which corresponds to a 10x increase in oscillation frequency when configured as a ring oscillator (Fig. 5). Our approach also allows valves to be repaired and reconfigured easily and reduces the number of valves needed to build digital logic circuits by introducing previously unreported pneumatic logic gates. These advances are expected to lead to expanded capabilities of soft robots and devices by broadening the suite of onboard control functionality without the need for tethering or incorporation of hard, electronic controllers.

4. Experimental Methods

Pressure Measurement. Experimental pressure measurements were taken when recording valve responses, snap-through pressures, regulator function, control glove pressures, piston force response, etc. In each experiment, a digital pressure sensor (ADP5151, Panasonic) was connected to every pressure location of interest (a valve input or output). To measure vacuum pressures, a separate sensor (ADP5101, Panasonic) was used. The electronic output of each sensor was measured using a central data acquisition device (USB-6002, National Instruments) before being converted to pressure values. When measuring the snap-through pressures of valves, we gradually increased the pressure input using a flow regulator (ITV0050-2BL, SMC). In the case of measuring negative snap-through pressures, a manually-operated

syringe was used to gradually create a vacuum. When measuring a decreasing pressure with no flow output (e.g., the decreasing output of a pressure regulator), we connected a pneumatic pull-down resistor (60 cm of thin tubing) to allow gradual pressure release.

Force-Displacement Characterization. The force-displacement relationships of internal valve components (shown in Fig. 2*B*) and the regulator input force (Fig. 4*B*) were acquired with a universal testing machine (68SC-2, Instron). Each valve component was secured in the testing machine before starting two cycles of extension and retraction, each 18 mm in length (or until 6 N was reached, in the case of the regulator). The force exerted by the component on the testing machine was recorded at each point in the second cycle.

Pressure-Mapping Measurement. The external pressure exerted by the cushion matrix (shown in Fig. 6) was measured using a pressure-mapping sensor (5250, TekScan). The cushion matrix was placed on top of the pressure-mapping sensor and constrained with flat surfaces on both sides before the spatial-pressure distribution was recorded.

Data, Materials, and Software Availability. All study data are included in the article and/or supporting information.

ACKNOWLEDGMENTS. This work was funded by Department of Energy award #DE-SC0000989 through a subcontract from Northwestern University; it is also based upon work supported by the National Science Foundation under Grant No. CMMI-2144809. C.J.D. acknowledges support from the Harvard Research Experience for Undergraduates (REU) program funded by the National Science Foundation under Grant No. DMR-2011754. A.R. acknowledges funding from the Rice University Academy of Fellows. Micro-CT imaging was performed in part at the Harvard University Center for Nanoscale Systems (CNS); a member of the National Nanotechnology Coordinated Infrastructure Network (NNCI), which is supported by the National Science Foundation under Grant No. ECCS-2025158. Mechanical testing was performed at the Robotics Core at Harvard John A. Paulson School of Engineering and Applied Sciences.

Author affiliations: [a]Department of Chemistry and Chemical Biology, Harvard University, Cambridge, MA 02138; [b]Department of Mechanical Engineering, Rice University, Houston, TX 77005; [c]Department of Robotics Engineering, Worcester Polytechnic Institute, Worcester, MA 01609; and [d]John A. Paulson School of Engineering and Applied Sciences, Harvard University, Cambridge, MA 02138

Author contributions: C.J.D., H.J.J., M.P.N., S.E.R., D.J.P., and G.M.W. designed research; C.J.D., H.J.J., M.P.N., A.R., J.T.A., J.T., and L.W. performed research; C.J.D., H.J.J., M.P.N., S.E.R., J.T.A., J.T., L.W. and D.J.P. contributed new reagents/analytic tools; C.J.D., H.J.J., S.E.R., A.R., J.T.A., J.T., L.W., D.J.P., and G.M.W. analyzed data; C.J.D., H.J.J., D.J.P., and G.M.W. wrote the paper; H.J.J. supervised C.J.D. in the Whitesides lab at Harvard University; M.P.N. supervised J.T. and L.W. in the Whitesides lab at Harvard University; A.R. supervised C.J.D. in the Preston lab at Rice University; D.J.P. oversaw the entire project, supervised the Preston lab at Rice University, and managed research resources; and G.M.W. initiated the general direction of research, oversaw the entire project, supervised the Whitesides lab at Harvard University, and managed research resources.

1. J. D. Hubbard *et al.*, Fully 3D-printed soft robots with integrated fluidic circuitry. *Sci. Adv.* **7**, eabe5257 (2021).
2. B. Mosadegh *et al.*, Pneumatic networks for soft robotics that actuate rapidly. *Adv. Funct. Mater.* **24**, 2163–2170 (2014).
3. D. Drotman, S. Jadhav, D. Sharp, C. Chan, M. T. Tolley, Electronics-free pneumatic circuits for controlling soft-legged robots. *Sci. Robot.* **6**, eaay2627 (2021).
4. D. J. Preston *et al.*, Digital logic for soft devices. *Proc. Natl. Acad. Sci. U.S.A.* **116**, 7750–7759 (2019).
5. P. Maeder-York *et al.*, Biologically inspired soft robot for thumb rehabilitation. *J. Med. Devices* **8**, 020933 (2014).
6. H. Wang, R. Zhang, W. Chen, X. Wang, R. Pfeifer, A cable-driven soft robot surgical system for cardiothoracic endoscopic surgery: Preclinical tests in animals. *Surg. Endosc.* **31**, 3152–3158 (2017).
7. K. C. Galloway *et al.*, Soft robotic grippers for biological sampling on deep reefs. *Soft Robot.* **3**, 23–33 (2016).
8. Y. Hao *et al.*, "Universal soft pneumatic robotic gripper with variable effective length" in *2016 35th Chinese Control Conference (CCC)* (2016), pp. 6109–6114.
9. A. T. Asbeck, R. J. Dyer, A. F. Larusson, C. J. Walsh, "Biologically-inspired soft exosuit" in *2013 IEEE 13th International Conference on Rehabilitation Robotics (ICORR)* (2013), pp. 1–8.
10. H. A. Sonar, A. P. Gerratt, S. P. Lacour, J. Paik, Closed-loop haptic feedback control using a self-sensing soft pneumatic actuator skin. *Soft Robot.* **7**, 22–29 (2020).
11. G. M. Whitesides, Soft robotics. *Angew. Chem. Int. Ed. Engl.* **57**, 4258–4273 (2018).
12. B. Jumet, M. D. Bell, V. Sanchez, D. J. Preston, A data-driven review of soft robotics. *Adv. Intell. Syst.*, **4**, 2100163.
13. T. C. Looney *et al.*, "Air-releasable soft robots for explosive ordnance disposal" in *2022 IEEE 5th International Conference on Soft Robotics (RoboSoft)* (2022), pp. 687–692.
14. A. Rajappan, B. Jumet, D. J. Preston, Pneumatic soft robots take a step toward autonomy. *Sci. Robot.* **6**, eabg6994 (2021).
15. E. W. Hawkes, C. Majidi, M. T. Tolley, Hard questions for soft robotics. *Sci. Robot.* **6**, eabg6049 (2021).
16. R. L. Truby, Designing soft robots as robotic materials. *Acc. Mater. Res.* **2**, 854–857 (2021).
17. P. Rothemund *et al.*, Shaping the future of robotics through materials innovation. *Nat. Mater.* **20**, 1582–1587 (2021).
18. A. Rajappan *et al.*, Logic-enabled textiles. *Proc. Natl. Acad. Sci. U.S.A.* **119**, e2202118119 (2022).
19. E. G. Hevia, L. De La Rochefoucauld, R. J. Wood, "Towards a microfluidic microcontroller circuit library for soft robots" in *2022 International Conference on Robotics and Automation (ICRA)* (2022), pp. 7138–7144.
20. B. Mosadegh *et al.*, Integrated elastomeric components for autonomous regulation of sequential and oscillatory flow switching in microfluidic devices. *Nat. Phys.* **6**, 433–437 (2010).
21. R. Z. Gao, C. L. Ren, Synergizing microfluidics with soft robotics: A perspective on miniaturization and future directions. *Biomicrofluidics* **15**, 011302 (2021).
22. T. Thorsen, S. J. Maerkl, S. R. Quake, Microfluidic large-scale integration. *Science* **298**, 580–584 (2002).
23. M. Wehner *et al.*, An integrated design and fabrication strategy for entirely soft, autonomous robots. *Nature* **536**, 451–455 (2016).
24. N. El-Atab, J. C. Canas, M. M. Hussain, Pressure-driven two-input 3D microfluidic logic gates. *Adv. Sci. (Weinh.)* **7**, 1903027 (2019).
25. P. N. Duncan, T. V. Nguyen, E. E. Hui, Pneumatic oscillator circuits for timing and control of integrated microfluidics. *Proc. Natl. Acad. Sci. U.S.A.* **110**, 18104–18109 (2013).
26. N. Pamme, Continuous flow separations in microfluidic devices. *Lab Chip* **7**, 1644–1659 (2007).
27. S. Song, S. Joshi, J. Paik, CMOS-inspired complementary fluidic circuits for soft robots. *Adv. Sci. (Weinh.)* **8**, e2100924 (2021).
28. J. A. Tracz *et al.*, Tube-balloon logic for the exploration of fluidic control elements. *IEEE Robot. Autom. Lett.* **7**, 5483–5488 (2022).
29. W.-K. Lee *et al.*, A buckling-sheet ring oscillator for electronics-free, multimodal locomotion. *Sci. Robot.* **7**, eabg5812 (2022).
30. P. Rothemund *et al.*, A soft, bistable valve for autonomous control of soft actuators. *Sci. Robot.* **3**, eaar7986 (2018).
31. D. J. Preston *et al.*, A soft ring oscillator. *Sci. Robot.* **4**, eaaw5496 (2019).
32. M. P. Nemitz *et al.*, "Soft non-volatile memory for non-electronic information storage in soft robots" in 2020 3rd IEEE International Conference on Soft Robotics (RoboSoft) (2020), pp. 7–12.
33. X. Jiang, P. B. Lillehoj, "Pneumatic microvalves fabricated by multi-material 3D printing" in 2017 IEEE 12th International Conference on Nano/Micro Engineered and Molecular Systems (NEMS) (2017), pp. 38–41.
34. E. Milana *et al.*, Morphological control of cilia-inspired asymmetric movements using nonlinear soft inflatable actuators. *Front. Robot. AI* **8**, 788067 (2022).
35. L. Jin, A. E. Forte, K. Bertoldi, Mechanical valves for on-board flow control of inflatable robots. *Adv. Sci. (Weinh.)* **8**, e2101941 (2021).
36. N. Vasios, A. J. Gross, S. Soifer, J. T. B. Overvelde, K. Bertoldi, Harnessing viscous flow to simplify the actuation of fluidic soft robots. *Soft Robot.* **7**, 1–9 (2020).
37. N. W. Bartlett, K. P. Becker, R. J. Wood, A fluidic demultiplexer for controlling large arrays of soft actuators. *Soft Matter* **16**, 5871–5877 (2020).
38. S. Hoang, K. Karydis, P. Brisk, W. H. Grover, A pneumatic random-access memory for controlling soft robots. *PLoS One* **16**, e0254524 (2021).
39. W. H. Grover, R. H. C. Ivester, E. C. Jensen, R. A. Mathies, Development and multiplexed control of latching pneumatic valves using microfluidic logical structures. *Lab Chip* **6**, 623–631 (2006).
40. R. A. Shveda *et al.*, A wearable textile-based pneumatic energy harvesting system for assistive robotics. *Sci. Adv.* **8**, eabo2418 (2022).
41. J. P. Whitney, M. F. Glisson, E. L. Brockmeyer, J. K. Hodgins, "A low-friction passive fluid transmission and fluid-tendon soft actuator" in *2014 IEEE/RSJ International Conference on Intelligent Robots and Systems* (2014), pp. 2801–2808.
42. J. Hepp, A. Badri-Spröwitz, A novel spider-inspired rotary-rolling diaphragm actuator with linear torque characteristic and high mechanical efficiency. *Soft Robot.* **9**, 364–375 (2022).
43. J. F. Taplin, "Flexible fluid sealing diaphragm." US Patent 2849026A (1958).
44. A. Gruebele, S. Frishman, M. R. Cutkosky, Long-stroke rolling diaphragm actuators for haptic display of forces in teleoperation. *IEEE Robot. Autom. Lett.* **4**, 1478–1484 (2019).
45. S. Hashemi, W. K. Durfee, "Low friction, long-stroke rolling diaphragm cylinder for passive hydraulic rehabilitation robots" in *2017 Design of Medical Devices Conference* (American Society of Mechanical Engineers, 2017), p. V001T05A016.
46. R. Feynman, *Feynman Lectures on Computation* (Addison-Wesley Longman Publishing Co., Inc., 1998).
47. S. V. Kendre *et al.*, The soft compiler: A web-based tool for the design of modular pneumatic circuits for soft robots. *IEEE Robot. Autom. Lett.* **7**, 6060–6066 (2022).
48. V. Sanchez, C. J. Walsh, R. J. Wood, Textile technology for soft robotic and autonomous garments. *Adv. Funct. Mater.* **31**, 2008278 (2021).
49. A. Yin, H.-C. Lin, J. Thelen, B. Mahner, T. Ranzani, Combining locomotion and grasping functionalities in soft robots. *Adv. Intell. Syst.* **1**, 1900089 (2019).
50. R. F. Shepherd *et al.*, Multigait soft robot. *Proc. Natl. Acad. Sci. U.S.A.* **108**, 20400–20403 (2011).
51. H. Hedayati, S. Bhaduri, T. Sumner, D. Szafir, M. D. Gross, "HugBot: A soft robot designed to give human-like hugs" in *Proceedings of the 18th ACM International Conference on Interaction Design and Children*, IDC '19, (Association for Computing Machinery, 2019), pp. 556–561.
52. A. E. Block, K. J. Kuchenbecker, "Emotionally supporting humans through robot hugs" in Companion of the 2018 ACM/IEEE International Conference on Human-Robot Interaction, HRI '18, (Association for Computing Machinery, 2018), pp. 293–294.
53. A. E. Block, K. J. Kuchenbecker, Softness, warmth, and responsiveness improve robot hugs. *Int. J. Soc. Robot.* **11**, 49–64 (2019).
54. Occupational Safety and Health Administration, *Facts About Hospital Worker Safety* (Occupational Safety and Health Administration, 2013).